NMR IN BIOMEDICINE
NMR Biomed. 1999;**12**:1–7

Diffusional anisotropy is induced by subcellular barriers in skeletal muscle†

Stephen T. Kinsey,[1]* Bruce R. Locke,[2,3]* Brigita Penke[3] and Timothy S. Moerland[2,4]

[1]University of North Carolina at Wilmington, Department of Biological Sciences, 601 South College Road, Wilmington, NC 28403-3297, USA
[2]Center for Interdisciplinary Magnetic Resonance, National High Magnetic Field Laboratory, 1800 E. Paul Dirac Drive, Tallahassee, FL 32310, USA
[3]Department of Chemical Engineering, FAMU-FSU College of Engineering, 2525 Pottsdamer Street, Tallahassee, FL 32307, USA
[4]Department of Biological Science, Florida State University, Tallahassee, FL 32306, USA

Received 20 January 1998; accepted 17 February 1998

ABSTRACT: The time- and orientational-dependence of phosphocreatine (PCr) diffusion was measured using pulsed-field gradient nuclear magnetic resonance (PFG-NMR) as a means of non-invasively probing the intracellular diffusive barriers of skeletal muscle. Red and white skeletal muscle from fish was used because fish muscle cells are very large, which facilitates the examination of diffusional barriers in the intracellular environment, and because they have regions of very homogeneous fiber type. Fish were cold-acclimated (5 °C) to amplify the contrast between red and white fibers. Apparent diffusion coefficients, D, were measured axially, $D_{\parallel}$, and radially, $D_{\perp}$, in small muscle strips over a time course ranging from 12 to 700 ms. Radial diffusion was strongly time dependent in both fiber types, and D decreased with time until a steady-state value was reached at a diffusion time $\simeq$100 ms. Diffusion was also highly anisotropic, with $D_{\parallel}$ being higher than $D_{\perp}$ for all time points. The time scale over which changes in $D_{\perp}$ occurred indicated that the observed anisotropy was not a result of interactions with the thick and thin filament lattice of actin and myosin or restriction within the cylindrical sarcolemma, as has been previously suggested. Rather, the sarcoplasmic reticulum (SR) and mitochondria appear to be the principal intracellular structures that inhibit mobility in an orientation-dependent manner. This work is the first example of diffusional anisotropy induced by readily identifiable intracellular structures. Copyright © 1999 John Wiley & Sons, Ltd.

KEYWORDS: diffusion; muscle; creatine kinase; energy transport

INTRODUCTION

Restrictions to motion in the cytoplasm have important implications for our understanding of cellular biochemistry. The cytoplasm is known to be a complex and crowded medium consisting of soluble and bound macromolecules, fibrous cytoskeletal elements, and an array of membrane bound organelles.[1] A growing body of evidence has demonstrated that diffusion of macromolecules is significantly hindered in cells due to hydrodynamic interactions with barriers such as the cytoskeletal network of fibroblasts[2–5] and the thick and thin filament array in muscle cells.[6,7]

These previous studies demonstrated the utility of using steady-state diffusion measurements of large tracer molecules, which were introduced into cells as probes of intracellular structure. However, small metabolites that occur naturally in cells provide a separate, non-invasive avenue for probing the barriers to diffusion in the cytoplasm. By measuring both the time- and orientational-dependence of diffusion of small metabolites, the length scales and orientation of diffusional barriers can be examined. Since the intracellular diffusion coefficients of metabolic substrates are 2–3 orders of magnitude greater than those of proteins, it is also likely that the mobility of substrates is of critical importance in generating protein–substrate interactions. Further, the barriers which are dominant in restricting the diffusion of small metabolites are very likely to be different from those which are dominant in restricting motion of macromolecules. For instance, it has recently been demonstrated that macromolecular probes are restricted from actin-rich regions of fibroblasts,[4] but this certainly would not be expected to be the case for small metabolites.

Previous studies have used water as a low-molecular weight probe of tissue structure, and diffusional aniso-

**Correspondence to:* S. T. Kinsey, University of North Carolina at Wilmington, Department of Biological Sciences, 601 South College Road, Wilmington, NC 28403-3297, USA
Contract/grant sponsor: National Institutes of Health postdoctoral fellowship; *contract grant number:* F32-DKO9571-01
Abbreviations used: ADP, adenosine diphosphate; ATP, adenosine triphosphate; BPP-LED, bipolar gradient pulse stimulated echo sequence with a longitudinal eddy current delay; CK, creatine kinase; ID, internal diameter; PCr, phosphocreatine; PFG-NMR, pulsed-field gradient nuclear magnetic resonance; SR, sarcoplasmic reticulum.

Copyright © 1999 John Wiley & Sons, Ltd.
CCC 0952–3480/99/010001–07 $17.50

tropy has been found in skeletal muscle,[8] cardiac muscle,[9,10] uterine muscle,[11] kidney,[12,13] and white matter.[14,15] However, water occurs in the intracellular, interstitial, and extracellular spaces, and knowledge of its diffusion yields little insight into intracellular structure. Water also readily crosses lipid membranes which further confounds the interpretation of *D*.

PCr is a substrate for the creatine kinase (CK; EC 2.7.3.2) reaction, which catalyzes the reversible transfer of a phosphoryl group from PCr to ADP, forming ATP. Mobility of PCr in muscle cells has been measured and, like other metabolites, has an apparent diffusivity that is reduced by about 40% from that measured in isotropic solutions.[16–18] PCr is an exceptional natural probe of the cytoplasmic barriers that cause this reduction in *D* because it is exclusively intracellular in skeletal muscle and its charged phosphoryl group restricts it from crossing lipid membranes. The time- and orientational-dependence of PCr mobility has been examined in skeletal muscle from rabbit hindlimb in the context of the cell's cylindrical geometry, but fiber orientation could not be rigorously controlled and intracellular restrictions were not noted.[17]

We have examined with high resolution the time-dependence of $D_{\parallel}$ and $D_{\perp}$ of PCr in red and white skeletal muscle from cold-acclimated (5 °C) goldfish using PFG-NMR. Skeletal muscle is an ideal tissue for examining restricted diffusion because of the highly ordered and well described internal structure of the cells. Our use of very small superfused muscle strips (< 1.5 mm diameter) allowed rigorous control of the orientation of the fibers, which is usually impossible for measurements made in larger tissue preparations or *in vivo*. Fishes are excellent vertebrate models because the muscle cells are very large, which reduces the interaction of the diffusing species with the cell's outer membrane, and because fish offer regions of very homogeneous red or white fibers. We report that diffusion of PCr is time- and orientation-dependent as a result of readily identifiable *intracellular* structures.

METHODS

Specimens

Goldfish (*Carassius auratus*) were obtained from Pineland Plantation Fish Farm (Newton, GA) and housed in 1000 L tanks containing recirculating well water. Fish were acclimated to 5 °C for a minimum of 6 weeks prior to experimental use. They were maintained on a 12h:12h day:night cycle and fed fish pellets daily. Fish weighed approximately 200 g at dissection.

NMR Procedures

Fish were anesthetized with 100 mg/L tricaine methanesulfonate. Strips of either red or white skeletal muscle were dissected from the region immediately posterior to the operculum and placed in oxygenated goldfish ringer's solution.[19] Muscle strips were cut parallel to the fiber orientation and were trimmed to a diameter of approximately 1.5 mm and a length of 10–15 mm. The muscle preparation was tied at either end with 6-0 surgical silk and suspended in the center of a 1.9 mm ID glass capillary superfusion chamber housed in an NMR probe. The glass capillary was fitted with superfusion lines which were snaked through the bottom of the probe to a set of peristaltic pumps. Temperature of the superfused tissue was maintained at 20 °C via a Brinkman model RM6 recirculating water bath. The NMR probe had a horizontal, five-turn solenoidal radiofrequency coil (2.6 mm ID) tunable to ^{1}H and ^{31}P which surrounded the superfusion chamber.

Experiments were performed on a Bruker 600 DMX spectrometer interfaced with a 14 T vertically-oriented widebore (89 mm) magnet complete with *XYZ* imaging gradients (960 mT/m maximum strength). Data were acquired and processed using a Silicon Graphics Indigo workstation and Bruker X-Win NMR software. To measure *D* of PCr, ^{31}P-spectra were acquired at 242 MHz using a bipolar gradient pulse stimulated echo sequence, with a longitudinal eddy current delay (BPP-LED; 20–22). This sequence minimizes eddy-current induced artifacts and negates the background gradients generated from susceptibility contrast in heterogenous samples.[24] In an isotropic solution, the signal amplitude, *A*, is described by

$$\ln(A/A_0) = -q^2(\Delta - \delta/3 - \tau/2)D \qquad (1)$$

where A_o is the signal amplitude in the absence of diffusion weighting gradients. The magnitude of the motion-encoding wavevector q is defined as $2\pi q = \gamma G\delta$, where γ is the magnetogyric ratio, G is the gradient amplitude, and δ is the gradient duration (of each bipolar pair). The parameter Δ is the time between the leading edges of each gradient pair, and τ is the time between the end of each gradient and the next radiofrequency pulse. In restricted or porous media, the diffusion coefficient is time dependent requiring an additional slight correction to Δ in order to obtain the true diffusion time.[25]

To measure *D*, a series of spectra were collected with different values for *G*. In all experiments, δ was 2 ms, τ was 250 μs, the recycle time was 2 s, the eddy current delay was 20 ms, and spectra were collected in either 256 or 512 scans. Gradient strengths ranged from 100 to 960 mT/m and pre-emphasis was used to achieve square gradient pulses. For typical experiments, four data points were collected for each diffusion measurement (in some cases more points were used). Diffusion was measured at 13 diffusion times, which ranged from 12 to 700 ms. The

Copyright © 1999 John Wiley & Sons, Ltd.

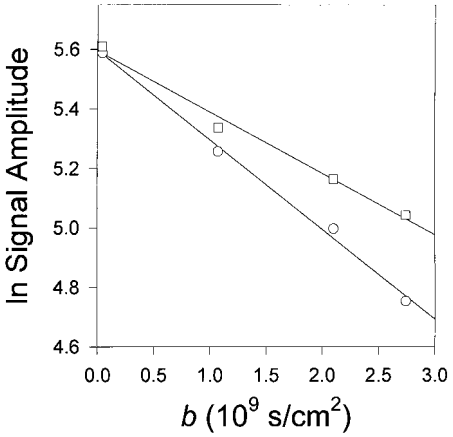

Figure 1. Typical attenuation plot of the PCr NMR signal as a function of the diffusion-weighting factor, *b*, for axial (circles) and radial (squares) diffusion in fish white muscle at a diffusion time of 100 ms. Faster attenuation is indicative of a higher *D*.

direction in which diffusion was measured was alternated for each diffusion time (e.g. $D_\perp$ was measured at 12 ms followed by measurement of $D_\parallel$ at 12 ms). Several determinations of *D* could be made for each tissue preparation. The bulk diffusion coefficient (D_0) of PCr was measured in a solution of 100 mM KCl, 2 mM monobasic KPO_4^-, 25 mM PCr, and 5 mM ATP at pH 7.4.

RESULTS

^{31}P-spectra demonstrated that the fish muscle preparations were maintained in an energetically favorable condition for periods >6 h as indicated by stability of the PCr and ATP peak areas. Experiments were conducted on fish only as long as PCr and ATP levels were >80% of their levels at the beginning of the experiments. This precaution and the fact that axial and radial measurements for a given time were conducted sequentially virtually eliminated the likelihood of systematic errors due to changes in the physiological condition of the tissues.

A typical plot of the PCr signal attenuation in muscle with increased *G* demonstrates the linearity found at all diffusion times (Fig. 1). At the shortest diffusion time ($\Delta = 12$ ms), the signal could only be attenuated by approximately 10%, because diffusion weighting is fairly low at these short times even at the maximum gradient intensity (960 mT/m) that could be achieved in our system. At times > 12 ms the signal could be attenuated more, and we maintained a constant maximal attenuation of approximately 60% for times from 50 to 700 ms.

Figure 2 demonstrates that both $D_\parallel$ and $D_\perp$ in muscle are substantially reduced at all diffusion times from the value measured in solution (D_0 of PCr in solution was found to be 5.56×10^{-6} cm^2/s $\pm$ 0.12, $n = 10$). $D_\perp$ was

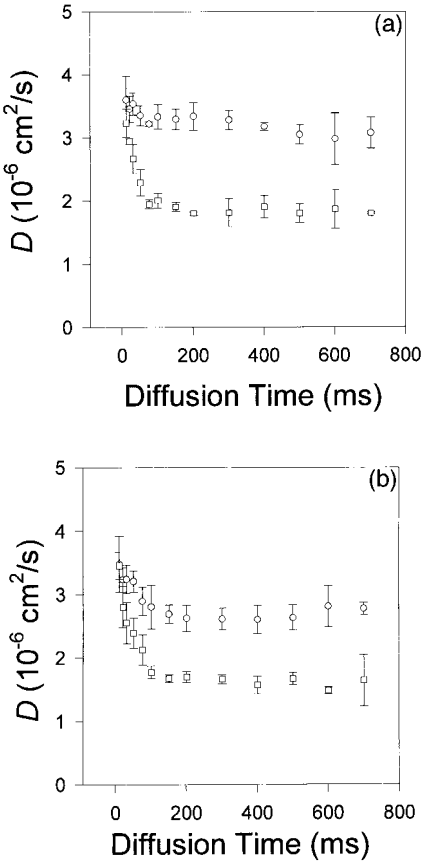

Figure 2. Time dependence of $D_\parallel$ (circles) and $D_\perp$ (squares) in: (a) white; and (b) red skeletal muscle strips of fish. Measurements are $D \pm$ s.e.m.

found to be strongly time-dependent and diffusion was highly anisotropic for both red and white skeletal muscle in fish. The time dependence occurs at diffusion times < 100 ms, afterwhich a steady-state long time diffusion coefficient is reached, as would be expected for diffusion through a porous medium. Although there is some reduction in $D_\parallel$ (particularly in red muscle), the hindrance to motion in the radial direction is much greater.

DISCUSSION

Diffusion of small metabolites through cells involves complex interactions of the diffusing species with soluble proteins and macromolecules, the cytoskeleton, and membranes. Modelling such processes is highly complex. However, for the purposes of demonstrating that we are observing the effects of intracellular barriers to motion, we can take advantage of the well ordered architecture of muscle to examine these barriers in isolation. In muscle cells, several dominant structural barriers are likely candidates to induce diffusional anisotropy: (1) the nm-scale myofilament lattice, which consists primarily of the

Copyright © 1999 John Wiley & Sons, Ltd.

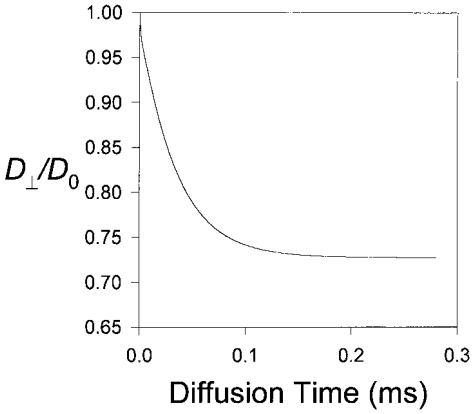

Figure 3. Time dependence of $D_\perp$ predicted for diffusion across an array of parallel cylindrical fibers representing the thick and thin filament lattice of muscle. A porosity of 0.86 was used based on the dimensions of the thick and thin filament array in muscle. D_0 was 5.6×10^{-6} cm^2/s as measured in bulk solution. See text for details.

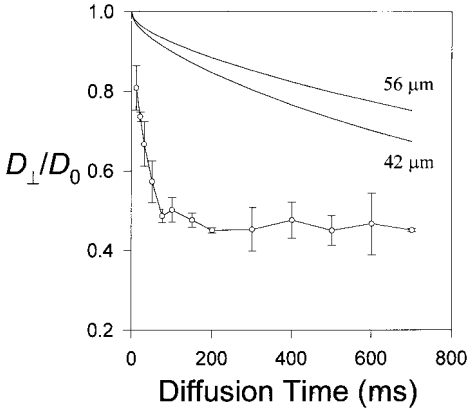

Figure 4. Time dependence of $D_\perp$ predicted for diffusion within a cylinder representing the sarcolemmal boundary of a muscle cell. The results are shown for diffusion in two cylinders of different radii plotted with the data for $D_\perp$ from fish white muscle. The radius of goldfish red muscle was 42.4 ± 14.1 μm and for white muscle 55.8 ± 19.8 μm. D_0 was estimated to be 4.0×10^{-6} cm^2/s as described in the text.

filamentous contractile proteins actin and myosin; (2) μm-scale subcellular membranes such as mitochondria and the SR; and (3) the 10^2 μm-scale sarcolemma, which is the cylindrical membrane that delineates individual muscle cells.

The time-dependence of $D_\perp$ through the nm-scale myofilament lattice can be approximated using volume averaging.[26] The formal solution for $D_\perp$ in a multiphase system leads to an expression that relates $D_\perp$ to the solution of a closure problem in a single unit (a filament and its surrounding sarcoplasm) that describes the typical features of the entire myofilament lattice. A single filament can be approximated by a pair of concentric circles that represent each filament and its surrounding cytosol as viewed in cross-section. The inner circle represents the solute impermeable filament. The outer circle defines the sarcoplasm. Time dependence of $D_\perp$ can then be described by

$$D_\perp(t)/D_0 = \left(1 - \frac{2R}{(R+l)^2} f(R,t)\right) \qquad (2)$$

where t is the diffusion time, D_0 is the bulk diffusion in the sarcoplasm, R is the radius of the filament, and l is 1/2 the distance between adjacent filaments. The function f satisfies the transient one-dimensional diffusion equation in the radial direction, r, with boundary conditions $f = 0$ at $r = R + l$, and $\partial f/\partial r = -1$ at $r = R$, and with intial conditions, $f = 0$ at $t = 0$. Dimensions of the myofilament lattice in vertebrate skeletal muscle are well known, and yield a weighted average estimate of 0.86 for porosity. Figure 3 shows the expected time-dependence of $D_\perp$ that would result from interaction with the myofilament lattice. Although this model is an approximation, it shows unequivocally that the time-dependence of $D_\perp$ reaches a steady-state in < 0.3 ms. This is well before our earliest PGSE-NMR measurement of $D_\perp$ at 12 ms diffusion time (Figure 2), and it demonstrates the intuitively satisfying point that the spacing of the thick and thin filament lattice has too fine a length scale to account for the observed time-dependent reduction in $D_\perp$.

Similarly, we can examine diffusion of a molecule restricted within a cylinder to estimate the maximum possible effect of the sarcolemma on $D_\perp$. The cylindrical cells in our preparations have a diameter of 84.8 ± 28.1 μm ($n = 54$) in red muscle and 111.6 ± 39.5 μm ($n = 54$) in white muscle, and both cell types are several millimeters in length. Radial diffusion in a restricted cylinder of radius a (radius of a single muscle cell) is well described at long diffusion times by[22]

$$D_\perp = 4a^2/\Delta \qquad (3)$$

and at short times by[23]

$$D_\perp/D_0 = 1 - \frac{4}{3a\sqrt{\pi}}\sqrt{D_0\Delta} \qquad (4)$$

The global behavior of $D_\perp$ restricted in a single cylinder has been approximated by interpolating between the long- and short-time asymptotic behavior to yield[22]

$$D_\perp/D_0 = (1 + \frac{4}{3\sqrt{\pi}}\sqrt{D_0\Delta/a^2} - 1.81(D_0\Delta/a^2)^{0.81} + 4(D_0\Delta/a^2))^{-1} \qquad (5)$$

Figure 4 shows the expected behavior of $D_\perp$ for two values of a that correspond to goldfish muscle cell dimensions, where the value for D_0 has been estimated at 4.0×10^{-6} cm^2/s. This value was obtained by linearly extending the short time diffusion data in muscle as a function of the square-root of time to the ordinate. This

Copyright © 1999 John Wiley & Sons, Ltd.

simplification allows a better estimate of the effect of the sarcolemma on $D_\perp$ by effectively treating nm-scale interactions (including macromolecular crowding and the effects of the myofilament lattice) as if they induce an increase in the bulk viscosity. Figure 4 demonstrates that the effect of the cylindrical sarcolemma cannot account for the time dependence observed; the steady-state diffusion coefficient is reached at a much later time (>120 s as compared with approximately 100 ms in muscle). It is also certain that the effect on $D_\perp$ due to restriction by the sarcolemma is vastly overestimated in Fig. 4 because PCr certainly has an average $D_\perp \ll 4.0 \times 10^{-6}$ cm^2/s over length scales of tens of microns (Fig. 2). It has previously been demonstrated that the $D_\perp$ of PCr in rabbit hindlimb is time-dependent and anisotropic due to restriction of radial mobility by the sarcolemma.[17] However, these authors calculated the diameter of the leg muscle cells from diffusion data to be $\simeq$17 μm, or five-fold smaller than the size of goldfish muscle cells.

It is clear that the diffusional anisotropy that we observed is a result of physical barriers with length scales much larger than the myofilament lattice, but well within the boundaries of the cells' sarcolemma. Mitochondria and SR both are logical candidates for the subcellular features responsible for this effect. Both have characteristic dimensions on the μm length scale and have a structural orientation that would be expected to induce the observed anisotropy. The SR is a reticulated membrane envelope that wraps around each myofibril or a bundle of 2–3 myofibrils. Each myofibril is $\simeq$1 μm in diameter, so the cylindrical partial membrane of the SR would serve as a strong barrier to radial diffusion, but would not be expected to hinder axial diffusion. The SR is well developed in both red and white muscle of goldfish, but it is more extensive in white muscle.[27] Mitochondria are interspersed between the myofibrils and, due to their oblate-spheroid shape, would be expected to restrict motion radially, and to a lesser extent, axially. Muscle from cold-acclimated goldfish (5 °C) provides a dramatic contrast, with mean free spacing between mitochondria roughly fifteen-fold greater in white muscle than in red muscle (68.7 and 4.7 μm, respectively; 27). Our results (Figure 2) show a rapid time-dependent decrease of $D_\perp$ in white muscle, but only a slight decrease in $D_\parallel$. This is consistent with the well developed SR and sparse mitochondria of white muscle. In red muscle, both $D_\perp$ and, to a lesser degree, $D_\parallel$ showed a time-dependent reduction. This is consistent with mobility being hindered radially by both the SR and mitochondria, and axially by mitochondria alone in this muscle type.

PCr is an exceptional natural probe of intracellular diffusion. Its highly charged phosphoryl group renders it impermeable to lipid membranes such as those of the SR, mitochondria, and sarcolemma, and it is exclusively intracellular. Both of these characteristics make PCr far superior to water as a probe of the intracellular environment. Further, the highly ordered and known structure of skeletal muscle make it possible to interpret diffusive behavior in terms of known features of the cellular architecture.

Our data show that diffusion of PCr in skeletal muscle is inherently anisotropic, and that the most reasonable interpretation of this is the presence of membranous structures such as the SR and mitochondria, which can comprise anisotropic barriers to diffusion. Magnetic resonance techniques are frequently employed to measure diffusion in tissues, and anisotropy is nearly always interpreted in terms of cell shape. This first example of diffusive anisotropy induced by *subcellular* barriers emphasizes the need to fully characterize orientation-specific constraints of intracellular diffusion in tissues, rather than simply making the assumption that the intracellular environment is isotropic.[28]

The reduction of $D_\perp$ also has implications for our understanding of intracellular energy transport in muscle. The cell biology of the creatine kinase system in which PCr is a substrate is complex, and there are several alternative views of its function.[29–31] Despite their differences, all functional interpretations of the creatine kinase system have the common feature that intracellular diffusion (axial and radial) of PCr over μm distances is the predominant means by which chemical potential energy is transported from the sites of ATP production (mitochondria) to the sites of its utilization (myosin ATPase; 31). Therefore, a key issue in understanding energy transport and integration of the processes of energy supply and demand in muscle is whether or not the diffusive flux of PCr (of which $D_\perp$ is a determinant) can be limiting for cellular function.

At least two lines of indirect evidence indicate that in most cases, intracellular diffusive flux of PCr from mitochondria to myofibrils is sufficient to meet the energy demands of active muscle. The first is the typical pattern of mitochondrial distribution in muscle, in which mitochondria are abundant at the fiber periphery ('subsarcolemmal' mitochondria) and present in low densities at the fiber core.[32] Kayar *et al.*[32] present a cogent argument that this distribution is a function of the diffusive mobility and flux rates of mitochondrial substrates and products: The predominance of subsarcolemmal mitochondria reflects the importance of short path lengths for diffusion of oxygen and other blood-borne substrates from capillaries to mitochondria, relative to the path lengths for intracellular diffusion of high-energy phosphates between mitochondria and myofibrils. Implicit in this is that radial diffusion of PCr from subsarcolemmal mitochondria to core myofibrils is sufficient. Second, quantitative models show that diffusion of phosphorous metabolites in muscle can be sufficient to avoid substantive intracellular gradients.[31,33] For example, our own reaction–diffusion analysis shows that [ATP], [PCr] and ΔG_{ATP} remain essentially constant

Copyright © 1999 John Wiley & Sons, Ltd.

across the diameter of goldfish red muscle fibers under conditions representative of maximal contractile activity.[34].

These models (including our own), however, have assumed isotropic intracellular diffusion. Our present results show that this is an oversimplification, and that accurate modeling of the CK reaction *in vivo* should account for restricted (i.e. time-dependent) radial diffusion of PCr. Refining models to incorporate restricted radial diffusion of PCr is likely to have little impact on the outcome for conditions representative of slow oxidative muscle, with small diameter cells, low rates of ATP utilization, and high mitochondrial capacities. In contrast, it may be important for larger diameter cells and/or higher rates of ATP demand: our reaction–diffusion analysis suggested that significant spatial and temporal gradients in [PCr] and ΔG_{ATP} develop in maximally active white fibers from goldfish, which have larger diameters, lower mitochondrial density, and higher rates of ATP demand than red muscle.[34] The magnitude of change in [PCr] and ΔG_{ATP} associated with these gradients may be large enough to lead to impaired contractile performance,[34] and the logical result of incorporating radial restrictions to PCr diffusion would be to exacerbate this effect. Additional evidence comes from the observation that the relative abundance of core ('intermyofibrillar') mitochondria in muscle can increase significantly in response to infrequent, high-intensity exercise.[32] These authors interpreted this as a compensatory response to reduce intracellular diffusion distances for exchange of phosphorous metabolites between mitochondria and myofibrils.[32] Similarly, Archer and Johnston[35] showed that the distribution of mitochondria in slow muscle of Antarctic fish is relatively homogeneous, which they interpreted as an adaptation to overcome thermal limitations to intracellular diffusion. Therefore, the restrictions to radial diffusion of PCr that we have demonstrated in this study may be a determinant of cellular organization in muscle in situations of high energy demand, low temperature, and/or long diffusion distances.

Acknowledgements

We thank Dr. Stephen Gibbs for his many insights during numerous discussions. This work was supported by a National Institutes of Health postdoctoral fellowship to S.T.K. while at the National High Magnetic Field Laboratory (F32-DK09571-01) and an American Heart Association Florida Affiliate Grant-in-Aid to T.S.M.

REFERENCES

1. Luby-Phelps K. Physical properties of cytoplasm. *Curr. Opin. Cell Biol.* **6**, 3–9 (1994).
2. Wojcieszyn J. W., Schlegel R. A., Wu E. -S. and Jacobson K. A. Diffusion of injected macromolecules within the cytoplasm of living cells. *Proc. Natl Acad. Sci. USA* **78**, 4407–4410 (1981).
3. Jacobson K. and Wojciezyn J. The translational mobility of substances within the cytoplasmic matrix. *Proc. Natl Acad. Sci. USA* **81**, 6747–6741 (1984).
4. Luby-Phelps K., Castle P. E., Taylor D. L. and Lanni F. Hindered diffusion of inert tracer particles in the cytoplasm of mouse 3T3 cells. *Proc. Natl Acad. Sci. USA* **84**, 4910–4913 (1987).
5. Janson L. W., Ragsdale K. and Luby-Phelps K. Mechanism of size cutoff for steric exclusion from actin-rich cytoplasmic domains. *Biophys. J.* **71**, 1228–1234 (1996).
6. Jurgens K. D., Peters T. and Gros G. Diffusivity of myoglobin in intact skeletal muscle cells. *Proc. Natl Acad. Sci. USA* **91**, 3829–3833 (1994).
7. Arrio-Dupont M., Cribier S., Foucault G., Devaux P. F. and d'Albis A. Diffusion of fluorescently labeled macromolecules in cultured muscle cells. *Biophys. J.* **70**, 2327–2332 (1996).
8. Cleveland G. G., Chang D. C., Hazlewood C. F. and Rorschach H. E. Nuclear magnetic resonance measurement of skeletal muscle. Anisotropy of the diffusion coefficient of the intracellular water. *Biophys. J.* **16**, 1043–1053 (1976).
9. Garrido L., Wedeen V. J., Kwong K. K., Spencer U. M. and Kantor H. L. Anisotropy of water diffusion in the myocardium of the rat. *Circ. Res.* **74**, 789–793 (1994).
10. Reese T. G., Weisskoff R. M., Smith R. N., Rosen R., Dinsmore R. E. and van Wedeen J. Imaging myocardial fiber architecture in vivo with magnetic resonance. *Magn. Reson. Med.* **34**, 786–791 (1995).
11. Yang Y., Xu S. and Dawson M. J. Measurement of water diffusion in hormone-treated rat uteri by diffusion-weighted magnetic resonance imaging. *Magn. Reson. Med.* **33**, 732–735 (1995).
12. Henkelman R. M., Stanisz G. J., Kim J. K. and Bronskill M. J. Anisotropy of NMR properties of tissues. *Magn. Reson. Med.* **32**, 592–601 (1994).
13. Muller M. F., Prasad P. V., Bimmler D., Kaiser A. and Edelman R. R. Functional imaging of the kidney by means of measurement of the apparent diffusion coefficient. *Radiology* **193**, 711–715 (1994).
14. Moseley M. E., Cohen Y., Kucharczyk J., Mintorovitch J., Asgari H. S., Wendland M. F., Tsudura J. and Norman D. Diffusion weighted MR imaging of anisotropic water diffusion in cat central nervous system. *Radiology* **176**, 439–445 (1990).
15. Moonen C. T. W., Pekar J., de Vleeschouwer M. H. M., van Gelderen P., van Zijl P. C. M. and Des Pres D. Restricted and anisotropic displacement of water in healthy cat brain and in stroke studied by NMR diffusion imaging. *Magn. Reson. Med.* **19**, 327–332 (1991).
16. Moonen C. T. W., van Zijl P. C. M., Le Bihan D. and DesPres D. *In vivo* NMR diffusion spectroscopy: ^{31}P application to phosphorus metabolites in muscle. *Magn. Reson. Med.* **13**, 467–477 (1990).
17. van Gelderen P., DesPres D., van Zijl P. C. M. and Moonen C. T. W. Evaluation of restricted diffusion in cylinders. Phosphocreatine in rabbit leg muscle. *J. Magn. Reson.* **103B**, 255–260 (1994).
18. Hubley M. J., Rosanske R. C. and Moerland T. S. Diffusion coefficients of ATP and creatine phosphate in isolated muscle: pulsed gradient ^{31}P NMR of small biological samples. *NMR Biomed.* **8**, 72–78 (1996).
19. Langfeld K. S., Crockford T. and Johnston I. A. Temperature acclimation in the common carp: force-velocity characteristics and myosin subunit composition of slow muscle fibres. *J. Exp. Biol.* **155**, 291–304 (1991).
20. Cotts R. M., Hoch M. J. R., Sun T. and Marker J. T. Pulsed field gradient stimulated echo methods for improved NMR diffusion measurements in heterogenous systems. *J. Magn. Reson.* **83**, 252–262 (1989).
21. Wu D., Chen A. and Johnson Jr. C. S. An improved diffusion-ordered spectroscopy experiment incorporating bipolar-gradient pulses. *J. Magn. Reson.* **115A**, 260–264 (1995).
22. Gibbs S. J. Observations of diffusive diffraction in a cylindrical pore by PFG NMR. *J. Magn. Res.* **124**, 223–226 (1997).
23. Mitra P. P., Sen P. N., Schwartz L. M. and Le Doussal P. Diffusion propagator as a probe of the structure of porous media. *Phys. Rev. Lett.* **68**, 3555–3558 (1992).
24. Trudeau J. D., Dixon W. T. and Hawkins J. The effect of inhomogeneous sample susceptibility on measured diffusion

Copyright © 1999 John Wiley & Sons, Ltd.

anisotropy using NMR imaging. *J. Magn. Reson.* **108B**, 22–30 (1995).
25. Fordham E. J., Mitra P. P. and Latour L. L. Effective diffusion times in multiple-pulse PFG diffusion measurements in porous media. *J. Magn. Reson.* **121A**, 187–192 (1996).
26. Carbonell R. G. and Whitaker S. Heat and Mass Transfer in Porous Media. In *Fundamentals of Transport Phenomena in Porous Media*, ed. by J. Bear and M. Y. Corapcioglu, pp. 121–198. Martinus Nijhoff Publishers, Dordrecht, 1984.
27. Tyler S. and Sidell B. D. Changes in mitochondrial distribution and diffusion distances in muscle of goldfish upon acclimation to warm and cold temperatures. *J. Exp. Zool.* **232**, 1 9 (1984).
28. Hsu E. W., Aiken N. R. and Blackband S. J. A study of diffusion isotropy in single neurons by using NMR microscopy. *Magn. Reson. Med.* **37**, 624–627 (1997).
29. Walliman T. M., Wyss M., Brdiczka D., Nicolay K. and Eppenberger H. M. Intracellular compartmentation, structure and function of creatine kinase isoenzymes in tissues with high fluctuating energy demands: the 'phosphocreatine circuit' for cellular energy homeostasis. *Biochem. J.* **281**, 21–40 (1992).
30. Bessman S. P. and Geiger P. J. Transport of energy in muscle: the phosphorylcreatine shuttle. *Science* **211**, 448–452 (1981).
31. Meyer R. A., Sweeney H. L. and Kushmerick M. J. A simple analysis of of the 'phosphocreatine shuttle'. *Am. J. Physiol.* **246**, C365–C377 (1984).
32. Kayar S. R., Claassen H., Hoppeler H. and Weibel E. R. Mitochondrial distribution in relation to changes in muscle metabolism in rat soleus. *Resp. Physiol.* **64**, 1–11 (1986).
33. Mainwood G. W. and Rakusan K. A model for intracellular energy transport. *Can. J. Physiol. Pharmacol.* **60**, 98–102 (1982).
34. Hubley M. J., Locke B. R. and Moerland T. S. Reaction–diffusion analysis of the effects of temperature on high-energy phosphate dynamics in goldfish skeletal muscle. *J. Exp. Biol.* **200**, 975–988 (1997).
35. Archer S. D. and Johnston I. A. Density of cristae and distribution of mitochondria in the slow muscle fibers of Antarctic fish. *Physiol. Zool.* **64**, 242–258 (1991).

Copyright © 1999 John Wiley & Sons, Ltd.